Molecular Microbiology (2011) 79(1), 50–62 ■
doi:10.1111/j.1365-2958.2010.07429.x
First published online 28 October 2010

Defining the role of a FYVE domain in the localization and activity of a cAMP phosphodiesterase implicated in osmoregulation in *Trypanosoma cruzi*

Alejandra C. Schoijet,[1,2,3] Kildare Miranda,[2,3,4] Lia Carolina Soares Medeiros,[3] Wanderley de Souza,[3,4] Mirtha M. Flawiá,[1,5] Héctor N. Torres,[1,5] Omar P. Pignataro,[6,7] Roberto Docampo[2,*] and Guillermo D. Alonso[1,5,]**

[1]*Instituto de Investigaciones en Ingeniería Genética y Biología Molecular, Consejo Nacional de Investigaciones Científicas y Técnicas, Vuelta de Obligado 2490, C1428ADN Buenos Aires, Argentina.*
[2]*Center for Tropical and Emerging Global Diseases and Department of Cellular Biology, University of Georgia, Athens, Georgia 30602, USA.*
[3]*Laboratório de Ultraestrutura Celular Hertha Meyer, Instituto de Biofísica Carlos Chagas Filho, and Instituto Nacional de Ciência e Tecnologia em Biologia Estrutural e Bioimagens, Universidade Federal do Rio de Janeiro, Brazil.*
[4]*Diretoria de Programas, Instituto Nacional de Metrologia, Normalização e Qualidade Industrial – INMETRO, Rio de Janeiro, Brazil.*
[5]*Departamento de Fisiología, Biología Molecular y Celular, Facultad de Ciencias Exactas y Naturales, Universidad de Buenos Aires, Buenos Aires, Argentina.*
[6]*Laboratorio de Endocrinología Molecular y Transducción de Señales, Instituto de Biología y Medicina Experimental, Consejo Nacional de Investigaciones Científicas y Técnicas, Vuelta de Obligado 2490, C1428ADN Buenos Aires, Argentina.*
[7]*Departamento de Química Biológica, Facultad de Ciencias Exactas y Naturales, Universidad de Buenos Aires, Buenos Aires, Argentina.*

Summary

Intracellular levels of cyclic nucleotide second messengers are regulated predominantly by a large superfamily of phosphodiesterases (PDEs). *Trypanosoma cruzi*, the causative agent of Chagas disease, encodes four different PDE families. One of these PDEs, *T. cruzi* PDE C2 (TcrPDEC2) has been characterized as a FYVE domain containing protein. Here, we report a novel role for TcrPDEC2 in osmoregulation in *T. cruzi* and reveal the relevance of its FYVE domain. Our data show that treatment of epimastigotes with TcrPDEC2 inhibitors improves their regulatory volume decrease, whereas cells overexpressing this enzyme are unaffected by the same inhibitors. Consistent with these results, TcrPDEC2 localizes to the contractile vacuole complex, showing strong labelling in the region corresponding to the spongiome. Furthermore, transgenic parasites overexpressing a truncated version of TcrPDEC2 without the FYVE domain show a failure in its targeting to the contractile vacuole complex and a marked decrease in PDE activity, supporting the importance of this domain to the localization and activity of TcrPDEC2. Taking together, the results here presented are consistent with the importance of the cyclic AMP signalling pathway in regulatory volume decrease and implicate TcrPDEC2 as a specifically localized PDE involved in osmoregulation in *T. cruzi*.

Accepted 5 October, 2010. For correspondence. *E-mail rdocampo@uga.edu; Tel. (+1) 706 542 8104; Fax (+1) 706 542 9493. **E-mail galonso@dna.uba.ar; Tel. (+54) 11 4783 2871; Fax (+54) 11 4786 8578.

Introduction

Degradation of the second messengers cAMP and cGMP is achieved through their hydrolysis by cyclic nucleotide phosphodiesterases (PDEs). Human Class I PDEs have been classified into 11 families based on sequence homology, enzymatic properties and sensitivity to inhibitors (Conti, 2000; Lugnier, 2001; Omori and Kotera, 2007). Given the complexity of the PDE families, it is now accepted that, although there may be some redundancy among isoenzymes, most of the different PDE variants play specific physiological functions (Bender and Beavo, 2006). In fact, PDEs can associate with other proteins, allowing them to be strategically anchored throughout the cell (Houslay and Adams, 2003; Cooper, 2005; Scott, 2006). In this regard, precise cellular expression and compartmentalization of these enzymes allows the specific control of cAMP gradients in cells and permits the integration with other signalling pathways (Baillie, 2009).

The data on the completed trypanosome genome (Berriman *et al*., 2005; El-Sayed *et al*., 2005; Ivens *et al*., 2005) have allowed the identification of four PDE families in *Trypanosoma cruzi, Trypanosoma brucei* and *Leishmania major*, which belong to the Class I PDEs. In trypanosomatids, cAMP is involved in the control of several processes including proliferation, cell differentiation, response to oxidative damage and osmoregulation (Flawia *et al*., 1997; Laxman and Beavo, 2007; Rohloff and Docampo, 2008; Bhattacharya *et al*., 2009). In *T. cruzi*, the aetiological agent of Chagas disease, previous studies on the response to hyposmotic stress have shown that both insect and vertebrate stages possess a strong regulatory volume decrease (RVD) mechanism that completely reverses cell swelling (Rohloff and Docampo, 2008). Moreover, it has been reported that cAMP levels increase when epimastigotes are subjected to hyposmotic stress, stimulating the traffic of an aquaporin from the acidocalcisomes to the contractile vacuole complex (CVC). Concomitantly, an increase in osmotically active metabolites occurs in the acidocalcisomes, which are transferred to the CVC creating an osmotic gradient that stimulates water entry into this organelle. Finally, the excess of water is released out of the cell through the flagellar pocket (Rohloff *et al*., 2004; Rohloff and Docampo, 2008). In this regard, the CVC, which is composed of a bladder and a series of numerous vesicles and tubules known as the spongiome, is a crucial organelle for the adaptation of this parasite to the osmotic fluctuations that occur throughout its life cycle.

Our laboratory has previously described three cAMP-specific PDEs in *T. cruzi*: TcrPDEB2, which was the first PDE cloned and biochemically characterized in this parasite and proved to be strongly associated to the flagellum (D'Angelo *et al*., 2004); TcrPDEA1, which was singularly resistant to the typical PDE inhibitors (Alonso *et al*., 2007); and TcrPDEC2, whose activity was associated to the membrane fraction in mutant yeast (Alonso *et al*., 2006). TcrPDEC2 has also been distinguished by the presence of a FYVE domain close to its N-terminus (amino acid positions 8–74). The FYVE domain is an approximately 60- to 70-amino-acid zinc binding finger involved in membrane trafficking, which specifically recognizes phosphatidylinositol 3-phosphate (PI 3-P) and recruits many proteins to PI 3-P enriched membranes (Kutateladze, 2007). The mechanism of membrane anchoring of the FYVE domain involves several features including non-specific electrostatic contacts with acidic lipids besides PI 3-P (Stahelin *et al*., 2002; Diraviyam *et al*., 2003; Kutateladze *et al*., 2004), hydrophobic insertion into the bilayers (Kutateladze and Overduin, 2001; Blatner *et al*., 2004) and in some cases oligomerization (Callaghan *et al*., 1999; Dumas *et al*., 2001). In addition, it has recently been reported that targeting of early endosome antigen 1 (EEA1) to PI 3-P membranes is also dependent on pH and regulated by a histidine switch (Lee *et al*., 2005).

Because of the correlation mentioned above between cAMP and osmoregulation, we studied the functional role of TcrPDEC2 in *T. cruzi*. We found that inhibition of TcrPDEC2 resulted in stimulation of the regulatory volume decrease after hyposmotic stress. Moreover, we demonstrated that TcrPDEC2 is localized to the CVC in epimastigotes of *T. cruzi* and revealed the importance of its FYVE domain for the subcellular targeting and catalytic activity of this enzyme.

Results

Characterization of pTREX-TcrPDEC2 transfected parasites

In order to investigate the role of TcrPDEC2 in *T. cruzi*, we overexpressed the TcrPDEC2 gene in epimastigotes. The pTREX-TcrPDEC2 construct was transfected into CL Brener epimastigotes generating stable cell lines after 60 days of selection with G418. The presence of an additional gene copy was confirmed by Southern blot analysis, where the extra hybridization bands observed in the pTREX-TcrPDEC2-expressing parasites indicate a successful integration of this construct (Fig. 1A). Northern blot analysis indicated significantly increased levels of the specific mRNA in the transfected parasites as compared with the wild-type cells (Fig. 1B). Additionally, the overexpression of TcrPDEC2 at the protein level was analysed by Western blot (Fig. 1C). As we reported previously (Alonso *et al*., 2006), a band with the expected apparent molecular weight (103 kDa) was detected in the membrane fraction (P100) in both wild-type and pTREX-TcrPDEC2-expressing parasite extracts using a polyclonal antiserum raised against the recombinant TcrPDEC2 expressed in *E. coli*. Moreover, a fourfold increase in the intensity of the band was observed in P100 extracts of transgenic versus wild-type parasites. Finally, PDE-specific activity was measured in P100 and S100 fractions of wild-type and pTREX-TcrPDEC2-expressing parasites (Fig. 1D). In agreement with the results obtained by Western blot analysis, TcrPDEC2 activity was mainly detected in the particulate fraction (Fig. 1D, black bars) and was 4.6-fold higher in extracts from pTREX-TcrPDEC2-expressing cells than in those from wild-type cells.

TcrPDEC2 is involved in volume recovery in epimastigotes

A previous report has shown that cAMP is involved in osmoregulation in *T. cruzi* and that intracellular levels of this second messenger increase when epimastigotes are subjected to hyposmotic stress (Rohloff *et al*., 2004). In

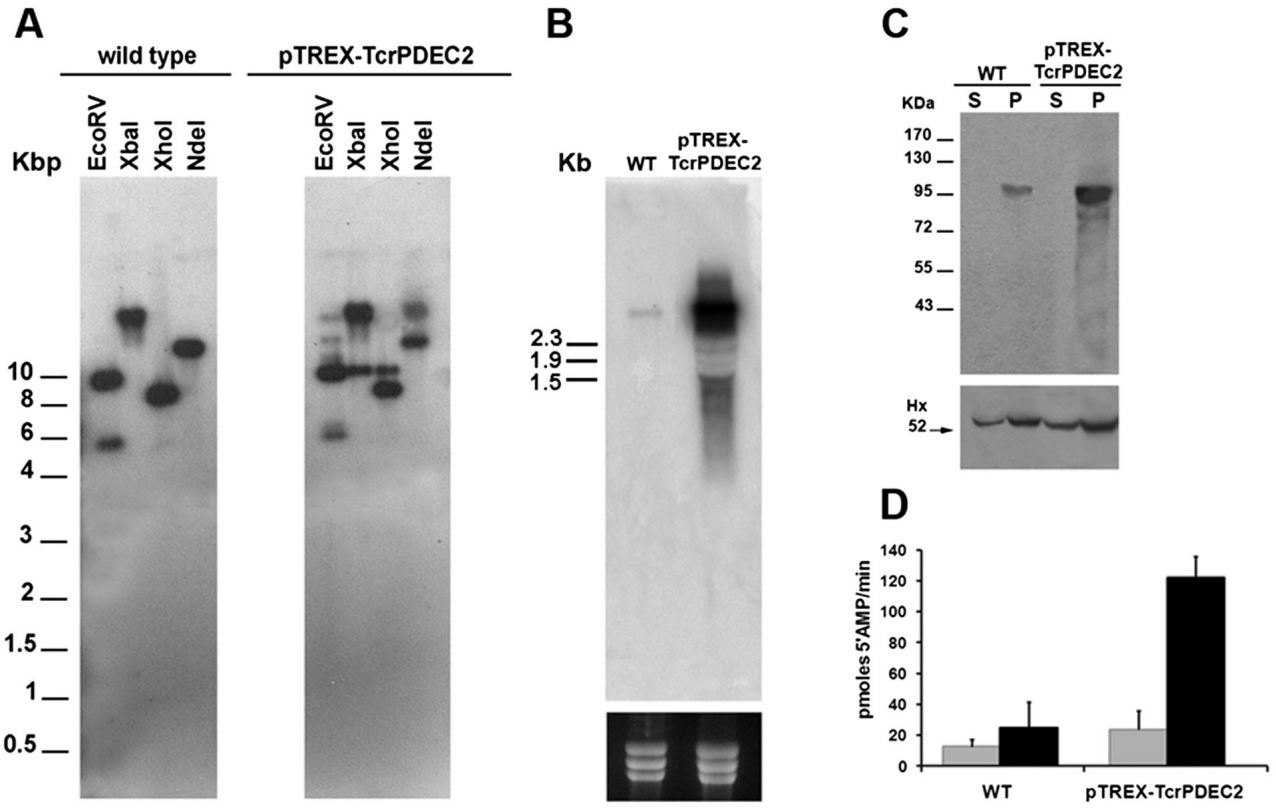

Fig. 1. Analysis of pTREX-TcrPDEC2-transfected parasites.
A. Southern blot analysis of wild-type and pTREX-TcrPDEC2 epimastigotes. Genomic DNA (5 μg) was digested with the following restriction endonucleases: EcoRV (that cuts in the position 833 of *TcrPDEC2* gene) and XbaI, XhoI or NdeI (which do not cut inside the *TcrPDEC2* gene). A radiolabelled 1070 bp fragment corresponding to the 5′ coding region of *TcrPDEC2* was used as a probe.
B. Northern blot analysis of wild-type and pTREX-TcrPDEC2 epimastigote cells. Total RNA (30 μg) from wild-type or pTREX-TcrPDEC2 transfected parasites were electrophoresed in agarose-formaldehyde gels, blotted and hybridized with the same probe described above. The migration position and loading control corresponding to the three ribosomal RNA bands are indicated.
C. Western blot analysis of wild-type and pTREX-*TcrPDEC2*-expressing epimastigotes. Proteins of S100 (S) or P100 (P) fractions (70 μg) were resolved by SDS-PAGE (8% gels), electrotransferred onto Hybond C membranes and revealed with anti-TcrPDEC2 antiserum. As control for loading amounts, the same membrane was blotted with anti-*T. cruzi* hexokinase antibody (bottom panel).
D. Enhanced cAMP phosphodiesterase activity in pTREX-TcrPDEC2-transfected parasites. PDE activity assays were performed as described under *Experimental procedures* using 30 μg of P100 (black bars) or S100 (gray bars) fractions of wild-type and pTREX-TcrPDEC2 parasites. Error bars represent the standard error of three experiments ($n = 3$).

addition, cAMP analogues stimulated volume recovery in epimastigotes (Rohloff *et al.*, 2004). To study whether TcrPDEC2 is involved in osmoregulation in *T. cruzi*, wild-type CL Brener and pTREX-TcrPDEC2-expressing epimastigotes were pre-incubated for 30 min with either 50 μM etazolate (triangles) or 50 μM rolipram (squares) and then subjected to hyposmotic stress (150 mOsm). Volume recovery was followed for 10 min by light scattering and compared with untreated controls (circles). As shown in Fig. 2A, etazolate and rolipram increased approximately 20% and 30%, respectively, the rate of recovery (defined under *Experimental procedures*) in wild-type cells. On the other hand, these inhibitors had no effect on pTREX-TcrPDEC2-expressing parasites (Fig. 2B). Additionally, wild-type cells treated with PDE inhibitors reached a final volume slightly lower than untreated cells. At the same time, approximately a 30% decrease in the rate of recovery of TcrPDEC2-overexpressing cells was observed as compared with wild-type cells [0.0116 ± 0.0015 (SEM) and 0.0171 ± 0.0028 (SEM) respectively, $n = 5$]. The treatment did not interfere with amino acid efflux, which still occurred, indicating that only the CVC contribution of the RVD was affected by the inhibitors. In addition, the integrity of the plasma membrane, evaluated by ethidium bromide uptake, was not affected during hyposmotic stress, excluding the possibility of toxic side-effects due to the treatment with these inhibitors (data not shown). Taken together, these results suggest an active role for TcrPDEC2 in the parasite response to hyposmotic stress. It is important to notice that no differences were observed when comparing wild-type cells with those transfected with pTREX-*GFP* vector (results not shown).

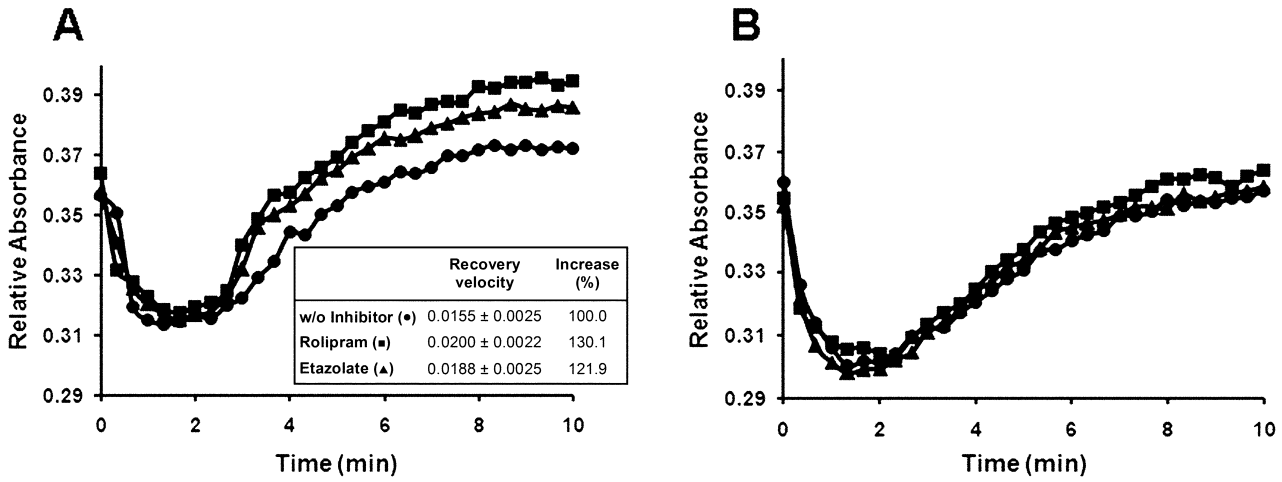

Fig. 2. Effect of TcrPDEC2 inhibitors on regulatory volume decrease. Wild-type (A) and transfected pTREX-TcrPDEC2-overexpressing cells (B) were pre-incubated with either 50 μM etazolate (*triangles*) or 50 μM rolipram (*squares*), and then subjected to hyposmotic stress. Relative changes in cell volume compared with untreated controls (*circles*) were followed by light scattering. Results are representative of those obtained from at least three independent experiments. (Inset in panel A) Table indicating the rate of recovery and the increase in the rate of recovery (%) in wild-type cells treated with etazolate, rolipram or without inhibitor (values are mean ± standard error corresponding to three independent experiments performed in triplicate).

To evaluate if the PDE inhibitors used could be affecting other PDEs, we investigated the *in vitro* PDE activity in wild-type and pTREX-TcrPDEC2-expressing parasite extracts in the presence of 50 μM etazolate or rolipram. According to the results of volume recovery, we observed that both compounds inhibited the PDE activity in wild-type cells [39.2% ± 0.91 (SEM) and 33.8% ± 1.1 (SEM) for etazolate and rolipram respectively], whereas they had a minor effect in pTREX-TcrPDEC2-expressing parasites [18.5% ± 2.0 (SEM) and 14.2% ± 1.8 (SEM) for etazolate and rolipram respectively].

TcrPDEC2 associates with the CVC in epimastigotes

In order to investigate the subcellular localization of TcrPDEC2, a fusion construct containing the enhanced GFP at the C-terminus of TcrPDEC2 was generated in pTEX vector (TcrPDEC2-GFP). Immunofluorescence microscopy of mid-log *T. cruzi* epimastigotes expressing this fusion protein showed a localization of TcrPDEC2-GFP in a region close to the flagellar pocket (Fig. 3B), which was similar to the localization observed when wild-type parasites were incubated with a specific antiserum against TcrPDEC2 (Anti-TcrPDEC2) generated in rabbit (Fig. 3D), suggesting that the TcrPDEC2-GFP pattern is not an artefact of protein overexpression and/or mistargeting. Since in trypanosomatids the flagellar pocket is located close to the CVC (Montalvetti *et al.*, 2004), we explored the possibility that TcrPDEC2 could be located in this latter structure in *T. cruzi*. Epimastigotes that were incubated with either an anti-TcrPDEC2 or an antiserum against calmodulin (Anti-CAM), a previously reported marker for the contractile vacuole (Zhu and Clarke, 1992; Rohloff *et al.*, 2004), showed colocalization of these proteins suggesting an association of TcrPDEC2 with the CVC (Fig. 3F–H). To further corroborate this result, we used epimastigotes expressing a version of TcAQP cloned in pTEX vector fused to the enhanced GFP at its C-terminal region, which serves as a suitable fluorescent marker for the contractile vacuole (TcAQP-GFP) (Montalvetti *et al.*, 2004). A strong colocalization of TcrPDEC2 with TcAQP-GFP in the contractile vacuole was detected (Fig. 3L), while no signal was observed when using the pre-immune serum or the secondary antibody alone (data not shown).

In all organisms examined to date, the CVC consists of a large central bladder surrounded by a diffuse radial network of tubules and vesicles known as the spongiome (Montalvetti *et al.*, 2004). To define the precise localization of TcrPDEC2 in the CVC, cryo-immunogold ultrastructural localization of this protein was performed in epimastigotes of *T. cruzi*. As Fig. 4 shows, most of the labelling was localized to the CVC with an accumulation at the spongiome vesicles and tubules that surround the bladder. Quantitative analysis of the particle density at the spongiome, bladder and cytosol, confirmed a higher density of TcrPDEC2 in the two first compartments, with prevalence in the spongiome (Fig. 4, right upper panel).

A functional FYVE domain is necessary for TcrPDEC2 catalytic activity

In addition to the PDE domain, TcrPDEC2 possesses a FYVE domain followed by two coiled-coil regions. A previous work has determined that the FYVE domain present

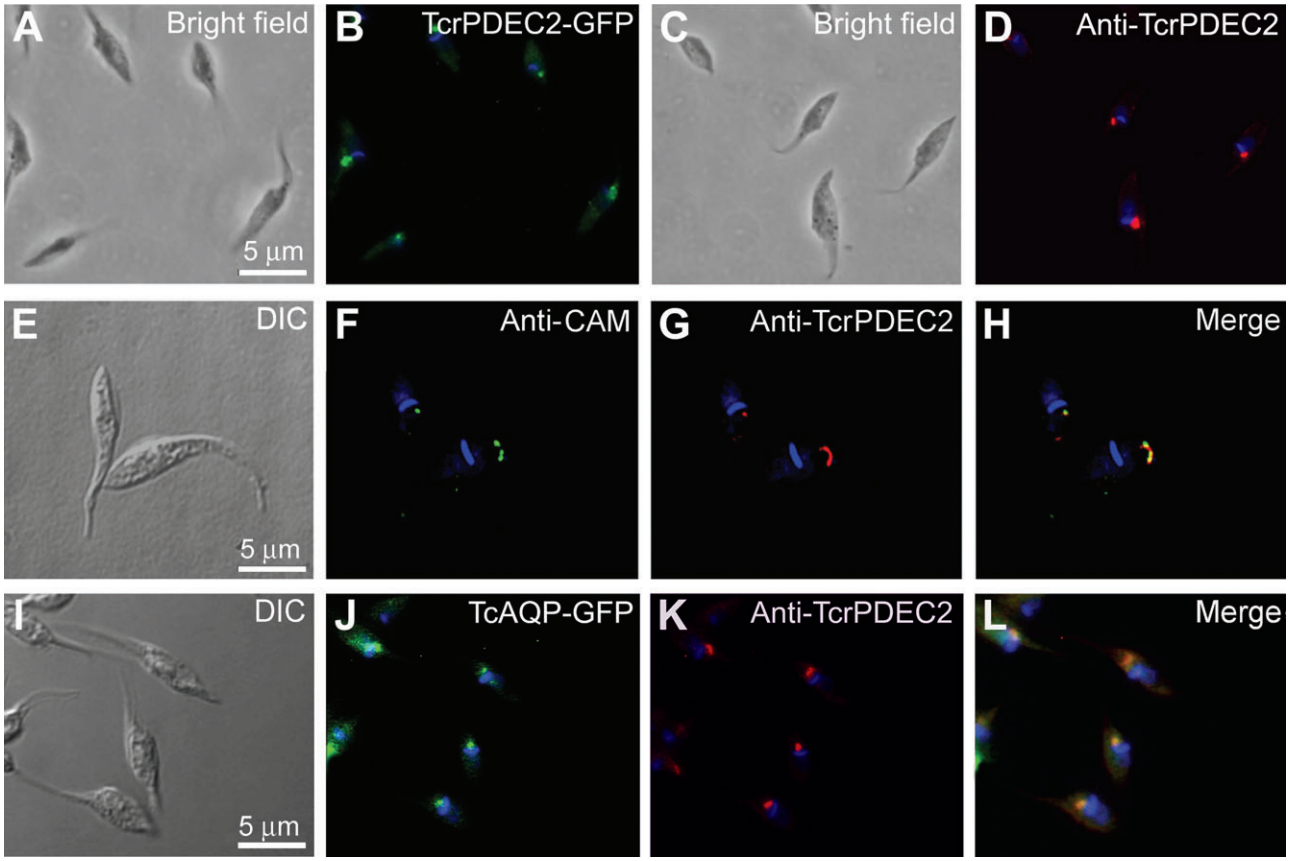

Fig. 3. Localization of TcrPDEC2 by immunofluorescence microscopy in epimastigotes of *T. cruzi*. Localization of TcrPDEC2-GFP (B) or endogenous TcrPDEC2 (D) revealed with antibodies against TcrPDEC2.
F–H. Colocalization of TcrPDEC2 (G) with a polyclonal antibody raised against a conserved N-terminal peptide from human calmodulin (F).
J–L. Colocalization of TcrPDEC2 (K) with TcAQP-GFP (J). (H) and (L) show the overlay of (F) and (G), and (J) and (K), respectively.
(A) and (C) are bright field images, and (E) and (I) are DIC images of the parasites. DAPI staining (blue) reveals the position of nuclear and kinetoplast DNA.

in TcrPDEC2 is a FYVE-variant domain that lacks some conserved residues. Although it has not been demonstrated, it could still bind PI 3-P, albeit with lower affinity than the classical FYVE domain (Kunz *et al*., 2005). This hypothesis is supported by the observation that the FYVE domain of TcrPDEC2 contains, among several conserved amino acids, the eight conserved cysteine residues predicted to be involved in zinc finger formation (Kunz *et al*., 2005). To further investigate if the FYVE domain of TcrPDEC2 is necessary for its catalytic activity, we overexpressed a truncated version of TcrPDEC2, with a deletion of 231 bp fragment corresponding to this domain, followed by a six-histidine tag. The correct integration of the pTREX-ΔFYVE-His construct was confirmed by Southern blot analysis (results not shown). Next, the expression at the RNA level was studied by Northern blot analysis and compared with that of wild-type cells and cells overexpressing the entire gene (pTREX-TcrPDEC2). As Fig. 5A shows, both specific mRNA levels in pTREX-ΔFYVE-His (ΔFYVE) and pTREX-TcrPDEC2 (TcrPDEC2) expressing cells were increased when compared with wild-type cells, revealing that the expression at the transcription level of this truncated version is not affected by the absence of the FYVE domain. Interestingly, when Western blot analysis was performed, a band corresponding to TrcPDEC2 was observed in the S100 fraction of pTREX-ΔFYVE-His-expressing parasites (Fig. 5B). Quantification of the intensity of the bands indicated that protein expression was 4.0-, 1.7- and 2.3-fold higher in pTREX-TcrPDEC2 P100, pTREX-ΔFYVE-His S100 and pTREX-ΔFYVE-His P100 fractions, respectively, than in the P100 fraction of wild-type parasites. Moreover, it is worth noticing that PDE activity in extracts of pTREX-ΔFYVE-His-expressing cells was significantly reduced when compared with extracts from cells overexpressing the entire protein (TcrPDEC2), showing values close to the observed in wild-type cells (Fig. 5C). The activity of the recombinant TcrPDEC2 was not affected by the presence of the His tag (results not shown) ruling out the possibility that the decreased activity was due to the presence of the tag. Since parasites

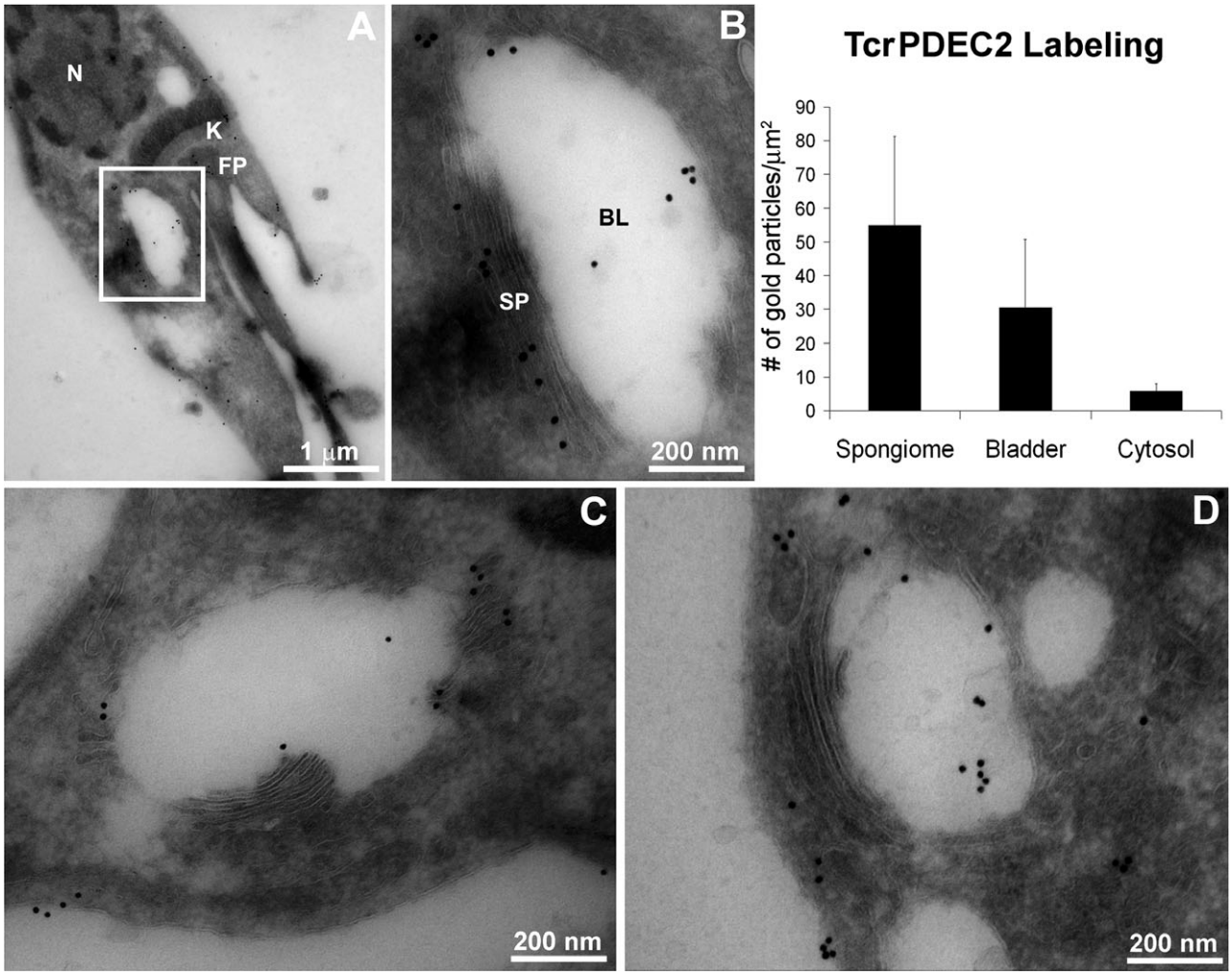

Fig. 4. Cryo-immunogold ultrastructural localization of TcrPDEC2 in epimastigotes.
A. Epimastigote forms were probed with an antiserum anti-TcrPDEC2. The square indicates the contractile vacuole complex.
B. Magnification of the region selected in (A). (C) and (D) are other magnifications showing in detail the contractile vacuole complex.
Abbreviations are: flagellar pocket (FP), kinetoplast (K), nucleus (N), spongiome (SP) and bladder (BL). The graphic shows the relative density distribution of TcrPDEC2 gold particles in the spongiome, bladder and cytosol.

overexpressing TcrPDEC2 had a slower rate of recovery after hyposmotic stress (Fig. 2B) and higher enzymatic activity (Fig. 5C) than control cells we investigated the intracellular levels of cAMP using a radioimmunoassay (RIA). Parasites overexpressing TcrPDEC2 had a 37.5% decrease in cAMP levels while the concentration of this cyclic nucleotide was not altered in the population that overexpresses the truncated version of this enzyme (pTREX-ΔFYVE-His) (Fig. 5D).

The localization of TcrPDEC2 to the CVC requires an intact FYVE domain

To investigate whether the FYVE domain is important for the subcellular localization of TcrPDEC2, we transfected parasites with the construct pTEX-ΔFYVE-GFP. We used pTEX instead of pTREX because this vector produces lower protein expression levels. Figure 6H shows a more diffuse and cytosolic localization of the GFP fluorescence than in controls expressing the full enzyme (Fig. 6C). Taken together, these results suggest that the FYVE domain is crucial both for the activity and the correct targeting of TcrPDEC2.

Discussion

Several fundamental cellular processes, such as membrane trafficking, cytoskeletal remodelling, endocytosis and cell survival, are regulated by subcellular targeting of key proteins which contain specific domains that bind to

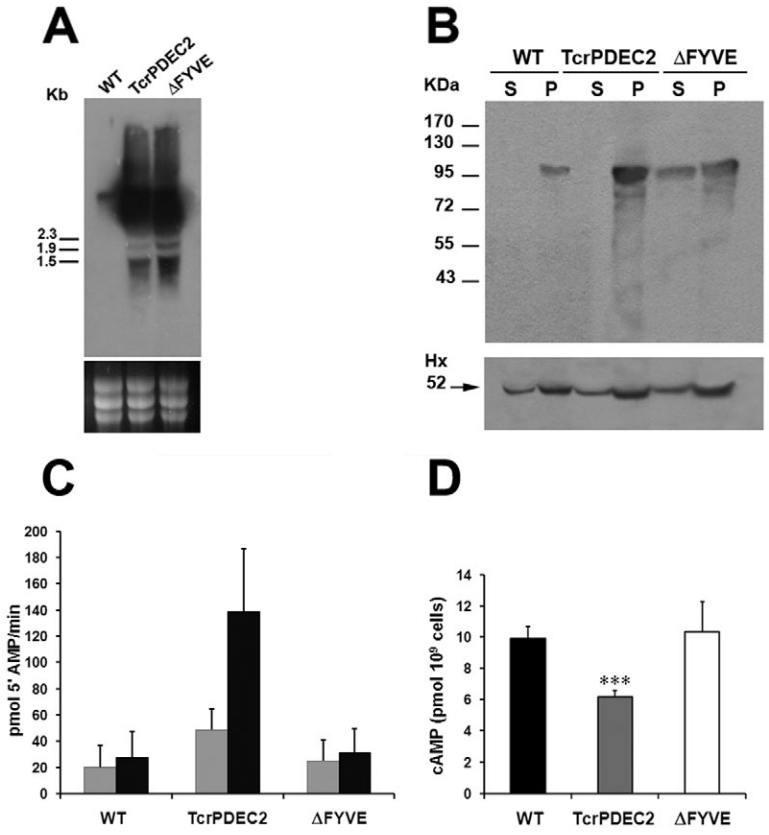

Fig. 5. Analysis of transgenic parasites lacking the FYVE domain.
A. Northern blot analysis of wild-type (WT), pTREX-TcrPDEC2 (TcrPDEC2) and pTREX-ΔFYVE-His (ΔFYVE) transfected parasites. Total RNA (30 μg) was electrophoresed in agarose-formaldehyde gels, blotted and hybridized with the same probe used in Fig. 1. The migration position and loading control corresponding to the three ribosomal RNA bands are indicated.
B. Western blot analysis of wild-type, pTREX-TcrPDEC2 and pTREX-ΔFYVE-His-expressing epimastigotes. Proteins of S100 (S) or P100 (P) fractions (70 μg) were resolved by SDS-PAGE (8% gels), electrotransferred onto Hybond C membranes and revealed with anti-TcrPDEC2 antiserum. The blot was sequentially probed with anti-*T. cruzi* hexokinase antibody as a loading control (bottom panel).
C. cAMP phosphodiesterase activity in transgenic parasites. PDE activity assays were performed as described under *Experimental procedures* using 30 μg of P100 (black bars) or S100 (grey bars) fractions of wild-type (WT), pTREX-TcrPDEC2 (TcrPDEC2) and pTREX-ΔFYVE-His (ΔFYVE) parasite extracts. Note that PDE activity in parasites lacking the FYVE domain is similar to the values obtained in wild-type parasites. Error bars represent the standard error of five experiments ($n = 5$).
D. Intracellular cyclic AMP levels in wild-type (WT), pTREX-*TcrPDEC2* (TcrPDEC2) and pTREX-Δ*FYVE-His* (ΔFYVE) expressing cells. There was a statistically significant (*t*-test, $P < 0.001$, *asterisks*) decrease in cyclic AMP levels in pTREX-TcrPDEC2 cells. Error bars represent the standard error of four experiments ($n = 4$).

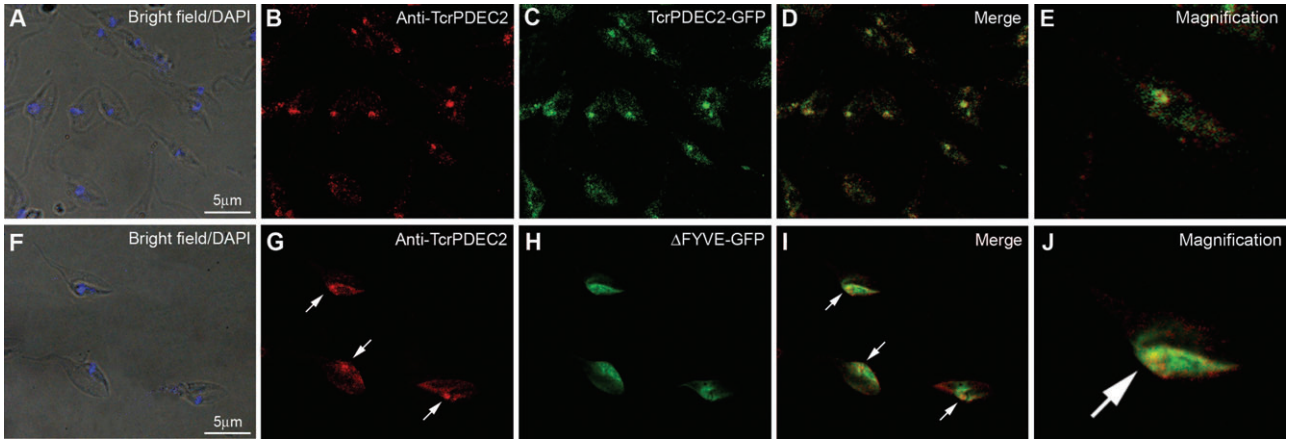

Fig. 6. The FYVE domain of TcrPDEC2 is required for its subcellular targeting. Immunofluorescence analysis of parasites lacking the FYVE domain (ΔFYVE-GFP) and parasites containing the entire protein (TcrPDEC2-GFP) used as control. The figure shows in green the localization of TcrPDEC2-GFP (C) and ΔFYVE-GFP (H), and in red, the same parasites labelled with the antiserum anti-TcrPDEC2 (B and G). (D) and (I) show the overlay of (B) and (C), and (G) and (H), respectively. Higher magnifications of representative cells are shown in (E) and (J). (A) and (F) are bright field images of the parasites plus the DAPI staining (blue) corresponding to the position of nuclear and kinetoplast DNA. The arrows in G and I show the contractile vacuole labelling.

phosphoinositides (Martin, 1998; Cullen *et al*., 2001; Payrastre *et al*., 2001), which are the phosphorylated derivatives of PI. Among these phosphoinositides, PI 3-P is localized mainly to endosomal membranes and internal vesicles of multivesicular bodies, but has also been detected in other compartments such as plasma membrane and Golgi, mitochondria and nucleus (Drobak and Heras, 2002; Kutateladze, 2007). This lipid is recognized principally by either PX or FYVE domains (Lemmon, 2003; Psachoulia and Sansom, 2009). Recently, Banerjee *et al*. (2010) reported that although both FYVE and PX domains bind to PI 3-P, the ligand binding specificity of PX is more versatile. Consequently, the authors found that in individual genomes PX domain-containing proteins are more abundant than FYVE-containing proteins. However, even though in protists does not seem to be selectivity for either FYVE or PX domains, it is worth noticing that the trypanosomatids *L. major, L. infantum, T. brucei* and *T. cruzi* have more FYVE domain-containing proteins (Banerjee *et al*., 2010).

The FYVE domain is an approximately 60- to 70-amino-acid motif that binds to the phosphoinositide PI 3-P with high specificity and affinity. It is present in 38 predicted gene products within the human genome, but only in 12–13 in *Caenorhabditis elegans* and *Drosophila melanogaster* (Hayakawa *et al*., 2007) and 19 in *T. cruzi* (Banerjee *et al*., 2010). Although Kunz *et al*. (2005) could not demonstrate that a fragment of TcrPDEC2 corresponding to its FYVE-variant domain alone was able to bind to phosphoinositides by using dot-spot assays, further studies are needed to understand the role of this domain in an intact protein context.

In order to investigate the role of TcrPDEC2 in *T. cruzi* epimastigotes, we generated TcrPDEC2-overexpressing parasites (pTREX-TcrPDEC2), which showed about five-fold more PDE activity in the particulate fraction than wild-type cells (Fig. 1D). Because the intracellular localization of PDEs is thought to be essential for compartmentalization of cyclic nucleotide-mediated processes (Houslay and Milligan, 1997; Baillie *et al*., 2005), we studied the subcellular localization of TcrPDEC2. For this purpose, we generated a GFP-tagged version of this protein that localized in a region near the flagellar pocket, which was coincident with the localization of the endogenous protein in wild-type parasites, assessed by using a specific antiserum (Fig. 3A–D). Moreover, TcrPDEC2 colocalized with calmodulin and TcAQP, two specific markers for the contractile vacuole complex (CVC) (Fig. 3H and L). Taking into account that the CVC is composed by a bladder and a network of vesicles and tubules known as the spongiome, to accurately determine the localization of TcrPDEC2 we performed cryo-immunogold electron microscopy experiments, establishing that this PDE is located mainly in the spongiome region (Fig. 4). However, it is worth mentioning that the signal was also detected on the bladder, indicating a dynamic membrane exchange between these compartments. It is known that the CVC is a key organelle involved in osmoregulation and that cAMP levels increase during hyposmotic stress in *T. cruzi* (Rohloff *et al*., 2004). Furthermore, Bao *et al*. have reported that the PKA catalytic subunit of *T. cruzi* (TcPKAc) interacts with TcrPDEC2 and two proteins implicated in osmoregulation: TcAQP and a class III phosphatidylinositol 3 kinase (TcVps34), among other proteins (Bao *et al*., 2008). Finally, the transcriptome analysis of the *T. cruzi* life cycle (Minning *et al*., 2009) has shown that TcrPDEC2 is highly expressed in metacyclic trypomastigotes, which is the stage that has to overcome a dramatic hyposmotic stress when transferred from the feces of the vector (> 600 mOsm) to the vertebrate host tissues (~330 mOsm). Based on these data, we hypothesized that TcrPDEC2 could be implicated in osmotic stress response, regulating the local levels of this second messenger.

Interestingly, when the RVD mechanism was evaluated either in the presence or in the absence of TcrPDEC2 inhibitors, it was observed that the inhibition of this enzyme stimulated between 20 and 30% the volume recovery of *T. cruzi* epimastigotes after hyposmotic stress, suggesting the participation of TcrPDEC2 in osmoregulation in this parasite. The final volume reached after hyposmotic stress was slightly lower in wild-type cells treated with PDE inhibitors than in untreated cells. This effect could be due to a loss of the downregulation of cAMP signal caused by the inhibition of the PDE activity. Moreover, the variation of intracellular cAMP levels in wild-type, pTREX-TcrPDEC2 and pTREX-ΔFYVE-His-expressing parasites was directly determined by RIA, showing a significant decrease only in pTREX-TcrPDEC2-expressing parasites. These results correlated with the RVD results, and with the increased PDE activity. We have reported before that an amino acid efflux mechanism accounts for approximately 50% of the regulatory volume decrease in epimastigote, trypomastigote and amastigote stages submitted to hyposmotic stress (Rohloff *et al*., 2003) while K^+ efflux in epimastigotes accounts for only about 7% of the regulatory volume decrease (Rohloff and Docampo, 2008). Only the difference (about 40%) would be accounted for by the cyclic AMP-mediated CVC mechanism (Rohloff *et al*., 2004; Rohloff and Docampo, 2008). However, this mechanism could also be important under isosmotic conditions. In this regard, the contractile vacuole of epimastigotes has periodic contractions under isosmotic conditions with a pulsation period between 1 min and 1 min and 15 s (Clark, 1959). It is well established that in many species, such as *Paramecium*, a CVC is necessary to maintain their water balance under normal environmental conditions as well as during dramatic

changes in their environment (Allen *et al*., 2009). We recently reported that chemically validated inhibitors of TcrPDEC could be lethal to intracellular stages of the parasite under isosmotic conditions (King-Keller *et al*., 2010). On the basis of these results we propose that the cAMP signalling pathway is necessary not only to overcome dramatic changes in osmolarity but also under isosmotic steady-state conditions. It is tempting to speculate that TcrPDEC would be an important mechanism to control cAMP oscillations responsible for the periodic function of the CVC.

Class I PDEs have three functional domains, a catalytic core, a C-terminal conserved domain and an N-terminal domain that is involved in the regulation and subcellular localization of each different PDE (Conti and Beavo, 2007; Halpin, 2008). To further study the relevance of the localization of TcrPDEC2 at the CVC and the role of its FYVE domain in determining this targeting, we generated parasites overexpressing a truncated version of TcrPDEC2, which lacks its aforementioned domain (pTREX-Δ*FYVE*). While parasites overexpressing the full version of TcrPDEC2 (pTREX-*TcrPDEC2*) significantly enhanced their PDE activity in the membrane fraction, pTREX-ΔFYVE-expressing parasites showed no difference on PDE activity levels as compared with wild-type cells, both in soluble and particulate fractions (Fig. 5C). These results could be explained by the necessity of an interaction between TcrPDEC2 and a specific membrane for enzymatic activity or because the deletion mutant is not able to acquire the right folding in the absence of its N-terminal region. Moreover, pTEX-ΔFYVE-expressing parasites showed a diffuse cytosolic localization (Fig. 6). This result might suggest that the FYVE domain plays a role in determining the final localization of TcrPDEC2, although the presence of other signals that may contribute to the correct targeting of this protein cannot be ruled out. In this regard, it has been reported that the EEA1 requires both its FYVE domain and the interaction with the small GTPase Rab5 for its targeting to endosomal membranes (Simonsen *et al*., 1998; Lawe *et al*., 2000).

Previous reports have shown that cAMP plays a crucial role in osmoregulation in *T. cruzi*. In the present work we demonstrate that TcrPDEC2 is a key enzyme controlling the local cAMP levels at the CVC and therefore regulating the RVD process in epimastigotes of *T. cruzi*. Furthermore, we showed that the subcellular localization of TcrPDEC2 requires its N-terminal FYVE domain, which may also be necessary for its catalytic activity.

Experimental procedures

Chemicals and reagents

All radiochemicals used in this work were purchased from Dupont NEN Life Science Products (Boston, MA, USA) and restriction endonucleases were from New England Biolabs (Beverly, MA, USA). Bacto-tryptose and liver infusion were from Difco Laboratories (Detroit, MI, USA). Goat polyclonal antibody raised against an N-terminal 19-amino-acid peptide from human calmodulin was purchased from Santa Cruz Biotechnology (Santa Cruz, CA, USA). Goat anti-rabbit Alexa 488 nm conjugate and rabbit anti-goat Alexa 546 nm conjugate were from Molecular Probes. All other reagents were purchased from SIGMA Chemical (St Louis, MO, USA).

Cell cultures and extracts

Trypanosoma cruzi epimastigote forms (CL Brener strain) were cultured at 28°C for 7 days in LIT medium [5 g l^{-1} liver infusion, 5 g l^{-1} bacto-tryptose, 68 mM NaCl, 5.3 mM KCl, 22 mM Na_2PO_4, 0.2% (w/v) glucose, 0.002% (w/v) haemin] supplemented with 10% (v/v) newborn calf serum, 100 units ml^{-1} penicillin and 100 mg l^{-1} streptomycin. Cell viability was assessed by direct microscopic examination. For *T. cruzi* extracts, 10^8 epimastigotes were harvested by centrifugation at 1500 *g* for 10 min and washed twice with phosphate-buffered saline (PBS). Cell pellets were then resuspended in lysis buffer (50 mM HEPES buffer, pH 7.3, containing 0.01 mg ml^{-1} leupeptin, 25 U ml^{-1} aprotinin, 0.5 mM phenylmethylsulphonyl fluoride and 14 mM 2-mercaptoethanol), and lysed by six cycles of freezing in liquid N_2 and thawing at 4°C. The total extracts were further centrifuged for 1 h at 100 000 *g* to obtain particulate (P100) and soluble (S100) fractions.

Southern, Northern and Western blot analyses

Genomic DNA was purified as described by Pereira *et al*. (2000). Total cellular RNA was isolated from 10^8 epimastigotes in the exponential growth phase using TRIzol reagents, as described by the manufacturer (Invitrogen). Southern and Northern blot analyses were performed as described by Alonso *et al*. (2007). The products were revealed with a specific 1070 bp TcrPDEC2 probe obtained by digestion of the 2772 bp fragment with BamHI and SacII. All probes were labelled with [α-^{32}P]-dCTP using the Prime-a-Gene kit (Promega, Madison, WI, USA) following the manufacturer's instructions.

TcrPDEC2 antiserum was developed in rabbit by intraperitoneal immunization with 800 μg of recombinant protein, expressed in *E. coli*, plus Freund's adjuvant followed by two more subsequent injections every 15 days without Freund's adjuvant.

For Western blot analysis, proteins were solved in 8% (w/v) SDS-polyacrylamide gel electrophoresis as described by Laemmli (1970) and electrotransferred to Hybond-C membranes (Amersham Pharmacia Biotech, Piscataway, USA). The membranes were blocked with 5% (w/v) non-fat milk suspension in TBS-Tween for 2 h. After overnight incubation with 1:1000 dilution of the rabbit anti-TcrPDEC2 antiserum, detection was carried out by incubating with a 1:5000 dilution of a goat anti-rabbit IgG labelled with peroxidase (KPL, Gaithersburg, MA, USA). The latter was developed with the ECL PlusTM Western Blotting Detection System (NEN Life Science Products, Boston, MA, USA). The intensity of the

bands obtained was quantified using the Gene Tools Software of Syngene images capture systems. To control for sample loading, the blot was also probed with a 1:2500 dilution of rabbit anti-*T. cruzi* hexokinase (Caceres *et al*., 2003).

TcrPDEC2 constructs and parasite transfection

The constructs pTREX-*TcrPDEC2*, pTEX-*TcrPDEC2-GFP* and pTEX-Δ*FYVE-GFP* were generated by PCR amplification from *T. cruzi* genomic DNA using the primers PDEC2-Fw-pTrex-XbaI 5′-TCTAGAATGTCGGAGGACGCTGGGCTT-3′ and PDEC2-Rv-pTREX-XhoI 5′-CTCGAGTCAGCACTGCGTCAACAGAGT-3′; the primers PDEC2-Fw-pTEXGFP-BamHI 5′-GGATCCATGTCGGAGGACGCTGGGCTT-3′ and PDEC2-Rv-pTEXGFP-BamHI 5′-GGATCCGTGCACTGCGTCAACAGAGTGGT-3′; and the primers PDEC2-Fw-ΔFYVE-pTEXGFP-BamHI 5′-GGATCCATGCGGCGACGCGTGGAGCCGGA-3′ and PDEC2-Rv-pTEXGFP-BamHI 5′-GGATCCGTGCACTGCGTCAACAGAGTGGT-3′, respectively. The PCR products were then cloned into pGEM-T Easy plasmid and subcloned into the pTREX integration (Vazquez and Levin, 1999) or pTEX-GFP episomal (Wilkinson *et al*., 2002) expression vector as applicable. The truncated form of *TcrPDEC2* lacking the 231 bp fragment corresponding to the N-terminal FYVE domain and 6xHis tagged at its C-terminus (pTREX-Δ*FYVE-His*) was amplified from the construct pET22-*TcrPDEC2* by using the primers ΔFYVE-Fw-XbaI 5′-TCTAGAATGGTGGAGCCGGATGAGGGATCAT-3′ and pET-Rv-XbaI 5′-TCTAGACTTCCTTTCGGGCTTTGTTAGCA-3′. The full-length TcrPDEC2 tagged at its C-terminus with 6xHis (pTREX-*TcrPDEC2-His*) was amplified in the same way that pTREX-ΔFYVE-His but using the primers PDEC2-Fw-pTrex-XbaI and pET-Rv-XbaI. Both PCR products were then cloned into pGEM-T Easy plasmid and subcloned into the pTREX expression vector (for detail of the constructs see Fig. S1). *T. cruzi* epimastigotes of CL Brener strain were transfected as described previously (Vazquez and Levin, 1999). Parasites transfected with pTREX-*GFP* or pTEX-*GFP* constructs were monitored by fluorescence microscopy as selection controls. Stable cell lines were achieved after 60 days of treatment with 500 μg ml^{-1} of G418 (Gibco BRL, Carlsbad, CA, USA) and the transgenic condition was confirmed by Southern blot, Northern blot and PDE activity analyses. Selection of pTEX transfectants were carried out beginning with 100 μg ml^{-1} of G418 and once those cultures were stabilized and growing properly, G418 concentration was increased up to 500 μg ml^{-1}.

Regulatory volume decrease

Epimastigotes were collected and washed twice with isotonic chloride buffer (Iso-Cl buffer, 137 mM NaCl, 4 mM KCl, 1.5 mM KH_2PO_4, 8.5 mM Na_2PO_4, 20 mM HEPES, 11 mM glucose, 1 mM $CaCl_2$, 0.8 mM $MgSO_4$, pH 7.4). The osmolarity of the buffer was adjusted to 300 ± 5 mOsm as verified by an Advanced Instruments 3D3 Osmometer (Norwood, MA, USA). The washed cells were resuspended in Iso-Cl buffer to a cell density of 1×10^8 cells ml^{-1}. The cells were distributed in 96-well plates with 150 μl per well in triplicates and hyposmotic stress was induced by 1:1 dilution of cell suspension with sterile deionized water, resulting in a final osmolarity of 150 mOsm. The absorbance changes at 550 nm were recorded every 20 s for 10 min using a SpectraMax M2e plate reader (Molecular Devices) (Rohloff *et al*., 2003). To further study the recovery capability after hyposmotic stress, we defined the rate of recovery as the slope corresponding to the linear region of the curve, comprised between the maximum swelling (2.33 min) and the plateau where the parasites stabilized their volume (5.66 min).

Membrane integrity and amino acid release

After treatment with the inhibitors etazolate and rolipram, membrane integrity was determined by ethidium bromide exclusion as described by Rohloff *et al*. (2003). Total amino acid analysis of the cell extracts and the supernatant fraction of epimastigote cells exposed to hypotonic or isotonic buffer were determined as described before (Rohloff *et al*., 2003).

Immunofluorescence microscopy

For immunofluorescence, cells were fixed in 0.1 M sodium cacodylate buffer (pH 7.2) containing 4% paraformaldehyde and washed twice in Dulbecco's PBS, pH 7.2, adhered to poly-L-lysine-coated coverslips, and permeabilized for 2 min with 0.3% Triton X-100. Cells were blocked for 20 min in 50 mM NH_4Cl and 3% bovine serum albumin in PBS, pH 8.0, and incubated for 1 h with rabbit polyclonal anti-TcrPDEC2 at 1:1000 and goat polyclonal anti-calmodulin antibody (Santa Cruz Biotechnology) at 1:50. Cells were then washed in 3% bovine serum albumin, incubated with secondary antibodies anti-rabbit Alexa 546 at 1:500 and anti-goat Alexa 488 conjugate at 1:500 containing 5 μg ml^{-1} DAPI and mounted with Vectashield (Vector Laboratories). Cells were observed alternative in an Olympus IX-71 fluorescence microscope with a Photometrix $CoolSnap_{HQ}$ CCD (charge-coupled device) camera driven by Delta Vision software (Applied Precision), an Olympus BX41 fluorescence microscope or axioplan Zeiss microscope.

Cryo-immunogold electron microscopy

For cryo-immuno electron microscopy, cells were fixed in 0.1 M sodium cacodylate buffer (pH 7.2) containing 4% paraformaldehyde and 0.1% glutaraldehyde for 1 h at 4°C. Cells were washed twice in sodium cacodylate buffer, pelleted by centrifugation, embedded in 25% polyvinylpyrrolidone plus 2.3 M sucrose and frozen in liquid nitrogen. Thin sections of frozen cells were obtained using a Leica EM FC6 cryoultramicrotome. Sections were blocked for 30 min in 50 mM NH_4Cl and 3% bovine serum albumin in PBS, pH 8.0 and incubated with anti-TcrPDEC2 at 1:100 for 1 h followed by goat anti-rabbit 15 nm gold at 1:100.

cAMP phosphodiesterase assays

PDE activity was determinate as described previously (Alonso *et al*., 2007). The reactions were performed using

30 μg of P100 or S100 fractions of parasite extracts in the presence of 20 mM Tris-HCl, pH 7.5, 5 mM Mg^{2+} and 50 μM [^{3}H]cAMP. Incubations were carried out at 30°C for 20 min in a total volume of 100 μl. For inhibition studies, rolipram and etazolate were used at a final concentration of 50 μM. Results represent means ± standard error of three experiments ($n = 3$).

Determination of intracellular cAMP

Cells were suspended at a concentration of 5×10^7 cells ml^{-1} and incubated with 1 mM IBMX for 10 min in Dulbecco's PBS supplemented with 5 mM glucose. Then they were centrifuged, and resuspended in 100 μl of PBS and 400 μl of 50 mM sodium acetate, pH 5.5, preheated to 95°C. These samples were heated at 95°C for 5 min, centrifuged, and the supernatants collected and stored at –20°C. Samples and standards were acetylated and assayed by RIA using the method described previously (Del Punta *et al*., 1996; Mondillo *et al*., 2009).

Acknowledgements

We wish to thank Dr Sumana Banerjee, from Department of Biological Sciences, Indian Institute of Science Education and Research for helpful information about the GI numbers of FYVE and PX containing proteins in Trypanosomatids. This work was supported in part by the Consejo Nacional de Investigaciones Científicas y Técnicas (CONICET, Argentina), University of Buenos Aires (Argentina), Agencia Nacional de Promoción Científica y Tecnológica (Argentina) and the U.S. National Institute of Health (grant AI-68647 to R.D.). G.D.A., M.M.F., H.N.T and O.P.P. are members of the Scientific Investigator Career of CONICET, Argentina. A.C.S. is a fellow from the same institution and was supported in part by a training grant of the Ellison Medical Foundation to the Center for Tropical and Emerging Global Diseases. W.S., K.M. and L.C.S.M. were supported by MCT-CNPq and FAPERJ.

References

Allen, R.D., Tominaga, T., and Naitoh, Y. (2009) The contractile vacuole complex and cell volume regulation. In *Osmotic and Ionic Regulation*. Evans, D.H. (ed.). Boca Raton: CRC Press, Taylor & Francis Group, pp. 69–105.

Alonso, G.D., Schoijet, A.C., Torres, H.N., and Flawia, M.M. (2006) TcPDE4, a novel membrane-associated cAMP-specific phosphodiesterase from *Trypanosoma cruzi*. *Mol Biochem Parasitol* **145:** 40–49.

Alonso, G.D., Schoijet, A.C., Torres, H.N., and Flawia, M.M. (2007) TcrPDEA1, a cAMP-specific phosphodiesterase with atypical pharmacological properties from *Trypanosoma cruzi*. *Mol Biochem Parasitol* **152:** 72–79.

Baillie, G.S. (2009) Compartmentalized signalling: spatial regulation of cAMP by the action of compartmentalized phosphodiesterases. *FEBS J* **276:** 1790–1799.

Baillie, G.S., Scott, J.D., and Houslay, M.D. (2005) Compartmentalisation of phosphodiesterases and protein kinase A: opposites attract. *FEBS Lett* **579:** 3264–3270.

Banerjee, S., Basu, S., and Sarkar, S. (2010) Comparative genomics reveals selective distribution and domain organization of FYVE and PX domain proteins across eukaryotic lineages. *BMC Genomics* **11:** 83.

Bao, Y., Weiss, L.M., Braunstein, V.L., and Huang, H. (2008) Role of protein kinase A in *Trypanosoma cruzi*. *Infect Immun* **76:** 4757–4763.

Bender, A.T., and Beavo, J.A. (2006) Cyclic nucleotide phosphodiesterases: molecular regulation to clinical use. *Pharmacol Rev* **58:** 488–520.

Berriman, M., Ghedin, E., Hertz-Fowler, C., Blandin, G., Renauld, H., Bartholomeu, D.C., *et al*. (2005) The genome of the African trypanosome *Trypanosoma brucei*. *Science* **309:** 416–422.

Bhattacharya, A., Biswas, A., and Das, P.K. (2009) Role of a differentially expressed cAMP phosphodiesterase in regulating the induction of resistance against oxidative damage in *Leishmania donovani*. *Free Radic Biol Med* **47:** 1494–1506.

Blatner, N.R., Stahelin, R.V., Diraviyam, K., Hawkins, P.T., Hong, W., Murray, D., and Cho, W. (2004) The molecular basis of the differential subcellular localization of FYVE domains. *J Biol Chem* **279:** 53818–53827.

Caceres, A.J., Portillo, R., Acosta, H., Rosales, D., Quinones, W., Avilan, L., *et al*. (2003) Molecular and biochemical characterization of hexokinase from *Trypanosoma cruzi*. *Mol Biochem Parasitol* **126:** 251–262.

Callaghan, J., Simonsen, A., Gaullier, J.M., Toh, B.H., and Stenmark, H. (1999) The endosome fusion regulator early-endosomal autoantigen 1 (EEA1) is a dimer. *Biochem J* **338:** 539–543.

Clark, T.B. (1959) Comparative morphology of four genera of trypanosomatidae. *J Protozool* **6:** 227–232.

Conti, M. (2000) Phosphodiesterases and cyclic nucleotide signaling in endocrine cells. *Mol Endocrinol* **14:** 1317–1327.

Conti, M., and Beavo, J. (2007) Biochemistry and physiology of cyclic nucleotide phosphodiesterases: essential components in cyclic nucleotide signaling. *Annu Rev Biochem* **76:** 481–511.

Cooper, D.M. (2005) Compartmentalization of adenylate cyclase and cAMP signalling. *Biochem Soc Trans* **33:** 1319–1322.

Cullen, P.J., Cozier, G.E., Banting, G., and Mellor, H. (2001) Modular phosphoinositide-binding domains – their role in signalling and membrane trafficking. *Curr Biol* **11:** R882–R893.

D'Angelo, M.A., Sanguineti, S., Reece, J.M., Birnbaumer, L., Torres, H.N., and Flawia, M.M. (2004) Identification, characterization and subcellular localization of TcPDE1, a novel cAMP-specific phosphodiesterase from *Trypanosoma cruzi*. *Biochem J* **378:** 63–72.

Del Punta, K., Charreau, E.H., and Pignataro, O.P. (1996) Nitric oxide inhibits Leydig cell steroidogenesis. *Endocrinology* **137:** 5337–5343.

Diraviyam, K., Stahelin, R.V., Cho, W., and Murray, D. (2003) Computer modeling of the membrane interaction of FYVE domains. *J Mol Biol* **328:** 721–736.

Drobak, B.K., and Heras, B. (2002) Nuclear phosphoinositides could bring FYVE alive. *Trends Plant Sci* **7:** 132–138.

Dumas, J.J., Merithew, E., Sudharshan, E., Rajamani, D., Hayes, S., Lawe, D., *et al*. (2001) Multivalent endosome targeting by homodimeric EEA1. *Mol Cell* **8:** 947–958.

El-Sayed, N.M., Myler, P.J., Bartholomeu, D.C., Nilsson, D.,

Aggarwal, G., Tran, A.N., *et al*. (2005) The genome sequence of *Trypanosoma cruzi*, etiologic agent of Chagas disease. *Science* **309:** 409–415.

Flawia, M.M., Tellez-Inon, M.T., and Torres, H.N. (1997) Signal transduction mechanisms in *Trypanosoma cruzi*. *Parasitol Today* **13:** 30–33.

Halpin, D.M. (2008) ABCD of the phosphodiesterase family: interaction and differential activity in COPD. *Int J Chron Obstruct Pulmon Dis* **3:** 543–561.

Hayakawa, A., Hayes, S., Leonard, D., Lambright, D., and Corvera, S. (2007) Evolutionarily conserved structural and functional roles of the FYVE domain. *Biochem Soc Symp* 95–105.

Houslay, M.D., and Adams, D.R. (2003) PDE4 cAMP phosphodiesterases: modular enzymes that orchestrate signalling cross-talk, desensitization and compartmentalization. *Biochem J* **370:** 1–18.

Houslay, M.D., and Milligan, G. (1997) Tailoring cAMP-signalling responses through isoform multiplicity. *Trends Biochem Sci* **22:** 217–224.

Ivens, A.C., Peacock, C.S., Worthey, E.A., Murphy, L., Aggarwal, G., Berriman, M., *et al*. (2005) The genome of the kinetoplastid parasite, *Leishmania major*. *Science* **309:** 436–442.

King-Keller, S., Li, M., Smith, A., Zheng, S., Kaur, G., Yang, X., *et al*. (2010) Chemical validation of phosphodiesterase C as a chemotherapeutic target in *Trypanosoma cruzi*, the etiological agent of Chagas' disease. *Antimicrob Agents Chemother* **54:** 3738–3745.

Kunz, S., Oberholzer, M., and Seebeck, T. (2005) A FYVE-containing unusual cyclic nucleotide phosphodiesterase from *Trypanosoma cruzi*. *FEBS J* **272:** 6412–6422.

Kutateladze, T.G. (2007) Mechanistic similarities in docking of the FYVE and PX domains to phosphatidylinositol 3-phosphate containing membranes. *Prog Lipid Res* **46:** 315–327.

Kutateladze, T., and Overduin, M. (2001) Structural mechanism of endosome docking by the FYVE domain. *Science* **291:** 1793–1796.

Kutateladze, T.G., Capelluto, D.G., Ferguson, C.G., Cheever, M.L., Kutateladze, A.G., Prestwich, G.D., and Overduin, M. (2004) Multivalent mechanism of membrane insertion by the FYVE domain. *J Biol Chem* **279:** 3050–3057.

Laemmli, U.K. (1970) Cleavage of structural proteins during the assembly of the head of bacteriophage T4. *Nature* **227:** 680–685.

Lawe, D.C., Patki, V., Heller-Harrison, R., Lambright, D., and Corvera, S. (2000) The FYVE domain of early endosome antigen 1 is required for both phosphatidylinositol 3-phosphate and Rab5 binding. Critical role of this dual interaction for endosomal localization. *J Biol Chem* **275:** 3699–3705.

Laxman, S., and Beavo, J.A. (2007) Cyclic nucleotide signaling mechanisms in trypanosomes: possible targets for therapeutic agents. *Mol Interv* **7:** 203–215.

Lee, S.A., Eyeson, R., Cheever, M.L., Geng, J., Verkhusha, V.V., Burd, C., *et al*. (2005) Targeting of the FYVE domain to endosomal membranes is regulated by a histidine switch. *Proc Natl Acad Sci USA* **102:** 13052–13057.

Lemmon, M.A. (2003) Phosphoinositide recognition domains. *Traffic* **4:** 201–213.

Lugnier, C. (2001) Cyclic nucleotide phosphodiesterase families in intracellular signaling and diabetes. *Adv Exp Med Biol* **498:** 253–261.

Martin, T.F. (1998) Phosphoinositide lipids as signaling molecules: common themes for signal transduction, cytoskeletal regulation, and membrane trafficking. *Annu Rev Cell Dev Biol* **14:** 231–264.

Minning, T.A., Weatherly, D.B., Atwood, J., III, Orlando, R., and Tarleton, R.L. (2009) The steady-state transcriptome of the four major life-cycle stages of *Trypanosoma cruzi*. *BMC Genomics* **10:** 370.

Mondillo, C., Pagotto, R.M., Piotrkowski, B., Reche, C.G., Patrignani, Z.J., Cymeryng, C.B., and Pignataro, O.P. (2009) Involvement of nitric oxide synthase in the mechanism of histamine-induced inhibition of Leydig cell steroidogenesis via histamine receptor subtypes in Sprague-Dawley rats. *Biol Reprod* **80:** 144–152.

Montalvetti, A., Rohloff, P., and Docampo, R. (2004) A functional aquaporin co-localizes with the vacuolar proton pyrophosphatase to acidocalcisomes and the contractile vacuole complex of *Trypanosoma cruzi*. *J Biol Chem* **279:** 38673–38682.

Omori, K., and Kotera, J. (2007) Overview of PDEs and their regulation. *Circ Res* **100:** 309–327.

Payrastre, B., Missy, K., Giuriato, S., Bodin, S., Plantavid, M., and Gratacap, M. (2001) Phosphoinositides: key players in cell signalling, in time and space. *Cell Signal* **13:** 377–387.

Pereira, C.A., Alonso, G.D., Paveto, M.C., Iribarren, A., Cabanas, M.L., Torres, H.N., and Flawia, M.M. (2000) *Trypanosoma cruzi* arginine kinase characterization and cloning. A novel energetic pathway in protozoan parasites. *J Biol Chem* **275:** 1495–1501.

Psachoulia, E., and Sansom, M.S. (2009) PX- and FYVE-mediated interactions with membranes: simulation studies. *Biochemistry* **48:** 5090–5095.

Rohloff, P., and Docampo, R. (2008) A contractile vacuole complex is involved in osmoregulation in *Trypanosoma cruzi*. *Exp Parasitol* **118:** 17–24.

Rohloff, P., Rodrigues, C.O., and Docampo, R. (2003) Regulatory volume decrease in *Trypanosoma cruzi* involves amino acid efflux and changes in intracellular calcium. *Mol Biochem Parasitol* **126:** 219–230.

Rohloff, P., Montalvetti, A., and Docampo, R. (2004) Acidocalcisomes and the contractile vacuole complex are involved in osmoregulation in *Trypanosoma cruzi*. *J Biol Chem* **279:** 52270–52281.

Scott, J.D. (2006) Compartmentalized cAMP signalling: a personal perspective. *Biochem Soc Trans* **34:** 465–467.

Simonsen, A., Lippe, R., Christoforidis, S., Gaullier, J.M., Brech, A., Callaghan, J., *et al*. (1998) EEA1 links PI(3)K function to Rab5 regulation of endosome fusion. *Nature* **394:** 494–498.

Stahelin, R.V., Long, F., Diraviyam, K., Bruzik, K.S., Murray, D., and Cho, W. (2002) Phosphatidylinositol 3-phosphate induces the membrane penetration of the FYVE domains of Vps27p and Hrs. *J Biol Chem* **277:** 26379–26388.

Vazquez, M.P., and Levin, M.J. (1999) Functional analysis of the intergenic regions of TcP2beta gene loci allowed the construction of an improved *Trypanosoma cruzi* expression vector. *Gene* **239:** 217–225.

Wilkinson, S.R., Meyer, D.J., Taylor, M.C., Bromley, E.V., Miles, M.A., and Kelly, J.M. (2002) The *Trypanosoma cruzi* enzyme TcGPXI is a glycosomal peroxidase and can be linked to trypanothione reduction by glutathione or tryparedoxin. *J Biol Chem* **277:** 17062–17071.

Zhu, Q., and Clarke, M. (1992) Association of calmodulin and an unconventional myosin with the contractile vacuole complex of *Dictyostelium discoideum*. *J Cell Biol* **118:** 347–358.

Supporting information

Additional supporting information may be found in the online version of this article.

Please note: Wiley-Blackwell are not responsible for the content or functionality of any supporting materials supplied by the authors. Any queries (other than missing material) should be directed to the corresponding author for the article.